

Preparation of Composite Membranes via Interfacial Polyfunctional Condensation for Gas Separation Applications

YAW-TERNG CHERN* and LEO-WANG CHEN

Institute of Materials Science and Engineering, National Taiwan University, Taipei 10764, Republic of China

SYNOPSIS

Composite membranes were prepared by interfacial polycondensation of a water-soluble diamine (4,4'-methylene dianiline [MDA] or ethylene diamine [EDA]) with an organic solvent (hexane)-soluble 1,2,4,5-benzenetetracyl chloride (BTAC) on top of a porous polysulfone (PSF) support. For both the poly(BTAC-MDA) and poly(BTAC-EDA) composite film systems, the permselectivity of these films increases only slightly with an increasing number of coatings. The poly(BTAC-MDA) composite membranes are treated at 135°C in a nitrogen atmosphere for 4 h, and they have a high selectivity [$\alpha^*(\text{CO}_2/\text{CH}_4) = 20.51$] and permeability [$\bar{P}(\text{CO}_2) = 44.12$ Barrer]. This is due mainly to the great chain stiffness of the formed polyimide, which has high selectivity. The high permeability is due to a porous polysulfone support. The trend of the permeability for this composite film is $\bar{P}(\text{CO}_2) > \bar{P}(\text{O}_2) > \bar{P}(\text{N}_2) > \bar{P}(\text{CH}_4)$. In poly(BTAC-EDA) composite membranes, the permeation of different gases decreases in the order of $\bar{P}(\text{CO}_2) > \bar{P}(\text{O}_2) > \bar{P}(\text{CH}_4) > \bar{P}(\text{N}_2)$. As to the composite films being more permeable to CH_4 than to N_2 , this is probably due to the presence of a considerable quantity of aliphatic chains ($-\text{CH}_2-\text{CH}_2-$) in the poly(BTAC-EDA) composite film caused by its particularly excellent solubility for methane.

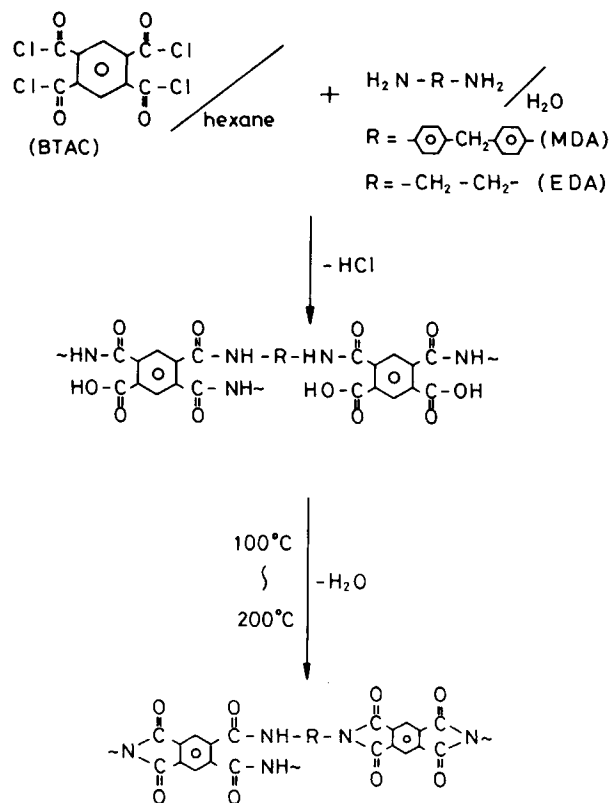
INTRODUCTION

Stiffer polymers generally have higher mobility-selectivity because they behave more like "molecular sieves."¹ Also, polymers with high glass transition temperature can bear high pressure without resulting in plastic deformation. They were considered important in the separation industry. Under high temperature, aromatic polyimide maintains excellent mechanical properties and chemical stability, so many researchers²⁻⁷ use polyimide as a separation membrane. Especially on separation of carbon dioxide and methane, polyimide has higher permselectivity than do other ordinary polymer films.³⁻⁷ However, the permeability of most polyimide membranes are not high; therefore, much research⁴⁻⁶ is being done in order to improve the permeation of polyimide membranes. This research covers structural al-

teration (by the substitution of side chains of appropriate bulkiness) that inhibits regular chain packing and simultaneously inhibits rotational motion about flexible linkages of the polymer backbone, thereby increasing permeability while maintaining or increasing selectivity⁴; structural alterations that promote sub- T_g motions while causing only small changes in intersegmental packing tend to increase permeability dramatically with tolerable changes in permselectivity.⁵

In previous studies,⁸⁻¹⁰ we discussed the interfacial polycondensation reaction in which BTAC was dissolved in an organic solvent and in which EDA or MDA were dissolved in water. We found that the film is formed by an interfacial polycondensation reaction and that the polyimide is formed upon thermal treatment. The typical reaction scheme is shown in Scheme 1. Also, the method of interfacial polycondensation can be applied for preparing composite membranes, providing high selectivity without severely reducing membrane flux.¹¹⁻¹⁴ These films prepared by interfacial polycondensation to

* To whom correspondence should be addressed.



Scheme 1

obtain composite membranes are used mainly for the reverse-osmosis desalination of sea water.^{13,14} For the preparation technique of polyimide membrane, the Loeb-Sourirajan procedure is mainly used. In previous research,¹⁵ we also prepared composite membranes by using interfacial polycondensation on top of a porous polysulfone support, and upon heat treatment, the polyimide composite membrane.

The gas permeation behavior of glassy polymers has been analyzed using the dual-mode transport model. This model takes dual-mode penetrants into account, i.e., gas molecules in Henry's law and Langmuir modes.^{16,17} The term Henry's law arises from the dissolution in the polymer matrix, while the term Langmuir arises from absorption in preexisting microvoids that are frozen in the polymer material below the glass transition temperature. For using polyimides as membrane material, there is a lot of research using the dual-mode transport model for analysis in order to calculate the solubility coefficient and diffusion coefficient of these films.^{18,19} However, because the composite membrane mentioned here is formed by two types of material and contains microporous support film, it may not be suitable to use the dual-mode transport model for

analysis. Therefore, in our research, we analyzed only the permeation coefficient, the chemical structure, and the morphology of composite membranes.

Fundamentals

The gas permeability of polymer membranes is characterized by a mean permeability coefficient, \bar{P} , which is defined by the isothermal relation^{1,4}

$$\bar{P} = \frac{G_s \times l}{(Ph - Pl) \times A} \quad (1)$$

where G_s is the steady-state rate of gas permeation through the effective area (A) of a membrane of thickness l , when the pressure Ph and Pl ($< Ph$) are maintained at the membrane interfaces. \bar{P} is reported in units of $\text{cm (STP) cm}^3/(\text{s cm}^2 \text{ cmHg})$.

The solution-diffusion process controlling transport through a polymer film leads to the relationship given in Eq. (2) among the mean permeability coefficient, \bar{P} , the mean diffusion coefficient, \bar{D} , and the solubility coefficient, S , for the gas in the polymer^{1,4}:

$$\bar{P} = S \times \bar{D} \quad (2)$$

To understand the factors affecting permeation, we can start from the individual factors affecting the diffusion coefficient and the solubility coefficient.²⁰ The diffusion coefficient is affected by the following factors: (1) the number and size distribution of preexisting holes, (2) the degree of ease of packing of the polymer chains, and (3) the ease of hole formation (relevant to the segment chain mobility, the chain stiffness, and the cohesive energy of the polymer). Beside these, the factors affecting the solubility coefficient are (1) the inherent condensibility of the penetrant gas, (2) the amount of excess volume existing, and (3) the polymer-penetrant interaction. From the above analysis, it can be understood that permeation is related to the nature of the penetrant gas and the polymer (relevant to morphology, chemical structure, molecular weight, molecular weight distribution, degree of branching, cross-linking, crystallinity, and plasticizing components) and the specific interaction between the gas and the polymer film.²⁰

The overall permselectivity of a membrane toward a gas A relative to another gas B is given by an "ideal separation factor" [$\alpha^*(A/B)$], which is defined by the relation^{1,4}

$$\alpha^*(A/B) = \frac{\bar{P}(A)}{\bar{P}(B)} \quad (3)$$

where $\bar{P}(A)$ and $\bar{P}(B)$ are the mean permeability coefficients for gases *A* and *B*.

EXPERIMENTAL

Materials

1,2,4,5-Benzenetetra acyl chloride (BTAC) was prepared from pyromellitic anhydride and phosphoric chloride.⁸ Methylene diamine (EDA) was recrystallized from isopropyl alcohol. Ethylene diamine (EDA) was distilled at normal pressure before use. Hexane was dried with 4 Å molecular sieves and was stored over molecular sieves until use. All the solvents used were purified in the usual manner. All other reagents were of analytical grade.

Preparation of Composite Membranes

To prepare the microporous polysulfone (PSF) substrate film, a 20% solution of PSF (Union Carbide Corporation, Grade P-3500) in dimethylformamide (DMF) was cast onto a flat glass plate using a 200 μm knife gap. The cast membrane was then gelled in a water bath at room temperature. The PSF film was prepared by methods described elsewhere.¹⁴ The PSF support was stored in deionized water until used. The top surface (air side) was used as the support surface for composite membrane formation.

The PSF support film prepared in the foregoing step was taken from deionized water. We wiped the surface (air side) of this support film dry with filter paper, before soaking the surface (air side) of the PSF support film in a culture dish containing the diamine (EDA or MDA) solution [as shown in Fig. 1(A)]. After soaking it for 10 min, we took out the PSF film. Excess solution was drained off the surface

by standing the PSF film up. The excess liquid was removed by using a piece of filter paper as a wick. The whole process takes 1 min. Next, we used rubber bands to fix the PSF film at the lower end of the glass tube (16 cm diameter) as shown in Figure 1(B). Then, we added 0.0061 *M* of BTAC solution (dissolved in hexane) to the PSF film by pouring it along the lining walls of the glass tube. Interfacial membrane synthesis was accomplished without stirring, using nondispersion methods. The organic solution was allowed to react for 5 min and the composite membrane was then taken from the glass tube. The composite membranes acquired by interfacial polycondensation were rinsed with 0.001 *N* of NaOH (aq), then rinsed with deionized water and methanol until no more dissolved substance appeared. Three rinses were required for each membrane. The above procedure for preparation of composite membranes was repeated to form a multilayer of composite membranes. Then, the membranes were vacuum-dried, and the dry membranes obtained were heated in a nitrogen atmosphere. The method for preparing composite film can eliminate the difficulty in the preparation of the composite film by interfacial condensation caused by the warping of the support film.

Analytical Procedures

Attenuated total reflectance (ATR) spectra were obtained on a Bomem MB 100 Fourier transform infrared spectrometer (FTIR) with 2 cm⁻¹ resolution, with KRS-5 used as an internal reflection element. Strips of supported film 5 × 0.5 cm² were placed on each side of the crystal so that the film surface was in contact with the crystal face. In a typical experiment, 200 scans per sample were av-

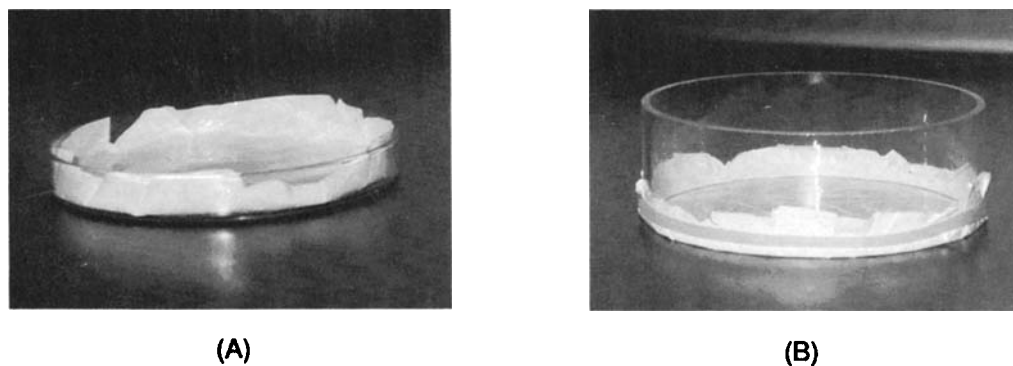


Figure 1 The preparation of composite membranes: (A) the film was laid in the culture dish; (B) the film was clamped on the glass frame ($D = 16$ cm).

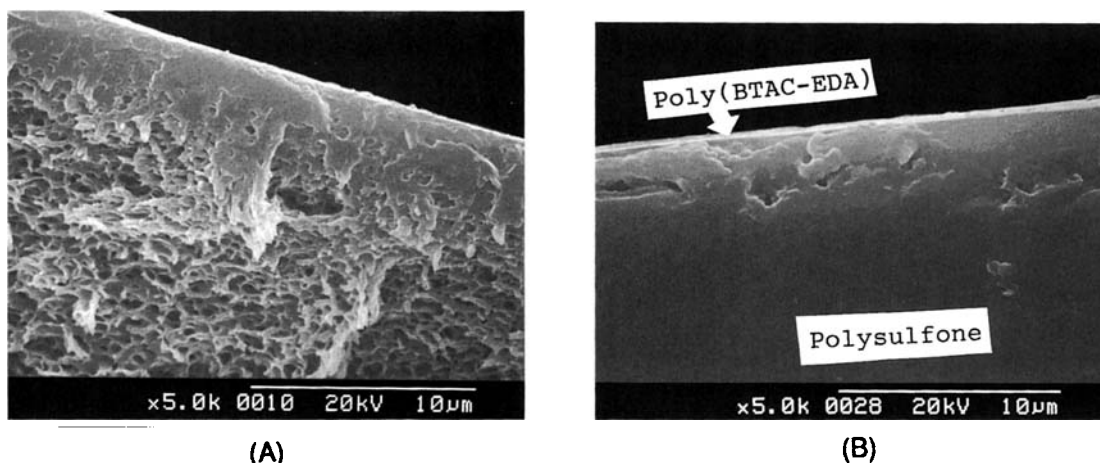


Figure 2 SEM photomicrographs of poly(BTAC-EDA) films supported with PSF: cross-section at (A) and (B). Thermal treatment: (A) before thermal treatment; (B) 6 h at 180°C.

eraged. The electron micrograph was taken with a Hitachi S-2300 scanning electron microscope. The polymer film was coated with gold by sputter deposition prior to the measurement.

Permeation measurements were performed on a Yanaco GTR-10 gas permeability analyzer (Yanaco New Science Inc., Kyoto, Japan) attached to a Yanaco G-2800T gas chromatograph (GC). The calibration gas was used as an external standard for the analysis of the permeant samples. A Yanaco G-2800T GC with thermal conductivity detector (TCD) was used for determining the concentration of permeant gas. Reproducibility, however, for truly identical samples is believed to be $\pm 3\text{--}4\%$. The composite membranes to be tested were placed between the two halves of a stainless-steel cell held together by bolts with two flat rubber gaskets to ensure a good seal. The effective area available for permeation is 15.2 cm^2 . The gases used in the study were $\geq 99.7\%$ pure. Only pure gas permeation results were measured.⁵ The permeation procedure is as follows: evacuation of a downstream side of the film up to about 0.05 mmHg, then introduction of permeant gas to an up-stream side. The pressure of the feed gas was controlled by a pressure-regulating valve with a pressure gauge. At the time, permeability measurement is started with the counting of measuring time. After the required time, gas permeated was introduced into the GC for determining the amount of permeant gas. We changed the measuring time and obtained the permeation amount from the different measuring time. The mean permeation coefficient is determined by the average value of the permeation coefficients obtained at three different times for each experiment.

RESULTS AND DISCUSSION

Morphology of the Composite Films

On comparison of the SEM photomicrographs of Figure 2(A) and (B), the photomicrograph of the latter one shows a nonporous morphology. The film was treated at 180°C, the temperature being close to the glass transition temperature of PSF ($T_g = 185^\circ\text{C}$),¹⁵ resulting in the movement of the chain segments to form a nonporous morphology. The detailed investigation for the morphology of composite membranes has been described elsewhere.¹⁵

Effect of the Number of Coatings on the Gas Permeability

On the whole, the permselectivity for the poly(BTAC-MDA) or poly(BTAC-EDA) composite film systems increases only slightly with an increasing number of coatings (Table 1). Therefore, we analyzed the permeation coefficient of composite films with one coating in our research below.

The Gas Permeability of the Nonheat-treated Composite Films

Referring to Table 2, for both poly(BTAC-EDA) and poly(BTAC-MDA) composite film systems, the permselectivity of the composite films decreases with a decreasing ratio of intensity of the amide absorption at 1640 cm^{-1} ($\text{C}=\text{O}$) and that of the acid at 1720 cm^{-1} ($\text{C}=\text{O}$). This is due to a decrease in the degree of cross-linking (containing less amide group)^{8,9}; therefore, the permselectivity decreases.

Table I Effect of the Number of Coatings on the Gas Permeability of Poly(BTAC-EDA) or Poly(BTAC-MDA) Films Supported with PSF at 28°C, with Upstream Pressure of 90.8 cmHg

Polymer	\bar{P}^a (CO ₂)	α^* (CO ₂ /CH ₄)	\bar{P}^a (O ₂)	α^* (O ₂ /N ₂)
Poly(BTAC-EDA) ^b	1438	0.87	1046	2.12
Poly(BTAC-EDA) ^c	1245	0.86	858	2.15
Poly(BTAC-MDA) ^b	1213	1.65	955	2.13
Poly(BTAC-MDA) ^c	1105	2.34	831	2.20

^a Barrer = 10⁻¹⁰ [cm³ (STP) cm/(s cm² cmHg)].

^b First coating.

^c Second coating.

As a whole, the permselectivity of the nonheat-treated composite films was low.

The Gas Permeability of the Heat-treated Poly(BTAC-MDA) Composite Films

Referring to Table 3, when the ratio of the intensity of the imide absorption at 1775 cm⁻¹ and that of the aromatic (C=C) at 1510 cm⁻¹ increases from 0 to 0.175, the α^* (CO₂/CH₄) value of the composite films increases from 1.65 to 20.51. The increase of permselectivity was attributed to two factors: (1) the softer chemical structure of amide originally contained in the composite films had mostly reacted to form a stiffer chemical structure of imide upon thermal treatment; and (2) the morphology of the composite films became more dense after thermal treatment.¹³ Stiffer polymers generally have a higher mobility (diffusivity) selectivity, because they behave more like "molecular sieves."¹ Such polymers

are better able to discriminate between penetrant molecules of different sizes and shapes. This is evident from the fact that the permeability of the poly(BTAC-MDA) composite film, treated at 135°C in a nitrogen atmosphere for 4 h (in Table 3), vs. different gases decreases in the order \bar{P} (CO₂) > \bar{P} (O₂) > \bar{P} (N₂) > \bar{P} (CH₄). This is also the order of increasing "kinetic" diameters²¹ of the penetrant molecules and commonly of decreasing diffusion coefficients of these gases in glassy polymers. Hence, the overall permselectivity of the poly(BTAC-MDA) composite film treated at 135°C in a nitrogen atmosphere for 4 h is probably controlled by the mobility selectivity.⁴ The increase of the α^* (O₂/N₂) value of the films was less than that of the α^* (CO₂/CH₄) value. This may be because the difference between the molecular kinetic diameter between CO₂ (3.3) and CH₄ (3.8) is greater, but is smaller between O₂ (3.46) and N₂ (3.64). The molecular sieving effect of a glassy polymer is greater the larger the difference in the size of the penetrant molecules.⁴ In Table 3,

Table II Effect of Chemical Structure on the Gas Permeability of Poly(BTAC-EDA) or Poly(BTAC-MDA) Films Supported with PSF at 28°C

Barrier Layer	Intensity Ratio ^a :		\bar{P}^b (CO ₂)	α^* (CO ₂ /CH ₄)	\bar{P}^b (O ₂)	α^* (O ₂ /N ₂)
	(Amide Band at 1640 cm ⁻¹)	(Acid Band at 1720 cm ⁻¹)				
None (bare PSF film)			1850	1.15	1750	1.51
Poly(BTAC-EDA) ^c	1.06		1438	0.87	1046	2.12
Poly(BTAC-EDA) ^d	1.03		1485	0.91	1081	1.89
Poly(BTAC-EDA) ^e	1.01		1496	1.08	1095	1.76
Poly(BTAC-MDA) ^c	1.13		1213	1.65	955	2.13
Poly(BTAC-MDA) ^d	1.04		1253	1.62	986	2.02
Poly(BTAC-MDA) ^e	0.98		1265	1.58	998	1.97

^a Calculated from the spectra of FTIR-ATR.

^b Barrer = 10⁻¹⁰ [cm³ (STP) cm/(s cm² cmHg)].

^c [BTAC] = [EDA] = 0.0061M; [BTAC] = [MDA] = 0.0061M.

^d [EDA]/[BTAC] = 0.9; [MDA]/[BTAC] = 0.9; [BTAC] = 0.0061M.

^e [EDA]/[BTAC] = 0.8; [MDA]/[BTAC] = 0.8; [BTAC] = 0.0061M.

Table III Effect of Imidization on the Gas Permeability of Poly(BTAC-MDA)^a Films Supported with PSF at 28°C

Barrier Layer	Intensity Ratio ^b :		\bar{P}^c (CO ₂)	α^* (CO ₂ /CH ₄)	\bar{P}^c (O ₂)	α^* (O ₂ /N ₂)
	$\left(\frac{\text{Imide Band at } 1775 \text{ cm}^{-1}}{\text{Aromatic C=C Band at } 1510 \text{ cm}^{-1}} \right)$					
Poly(BTAC-MDA)	0		1213	1.65	955	2.13
Poly(BTAC-MDA) ^d	0.009		1195	2.45	932	2.59
Poly(BTAC-MDA) ^e	0.175		44.12	20.51	17.73	2.65
Poly(BTAC-MDA) ^f	0.182		4.26	20.82	2.57	5.28

^a [MDA] = [BTAC] = 0.0061M.

^b Calculated from the spectra of FTIR-ATR.

^c Barrer = 10⁻¹⁰ [cm³ (STP) cm/(s cm² cmHg)].

^d Thermal treatment: 10 min at 150°C.

^e Thermal treatment: 4 h at 135°C.

^f Thermal treatment: 6 h at 180°C.

the α^* (O₂/N₂) value of the sample treated at 180°C in a nitrogen atmosphere for 6 h is increased after heat treatment. This is due mainly to the morphology of the composite films becoming nonporous.

The permeation coefficient for the poly(BTAC-MDA) composite film treated at 135°C in a nitrogen atmosphere for 4 h shown in Table 3 is about 10 times greater than in other polymers such as polyimide [\bar{P} (CO₂) = 4.03 Barrer for the PMDA-MDA system]. But, the α^* (CO₂/CH₄) value of the poly(BTAC-MDA) composite film system treated at 135°C in a nitrogen atmosphere for 4 h shown in Table 3 is about one-half of that of the other polyimide [α^* (CO₂/CH₄) = 42.9 for the PMDA-MDA system].²² This is probably because the poly(BTAC-MDA) composite film treated at 135°C in a nitrogen atmosphere for 4 h contained a microporous PSF support,¹⁵ making the permeation coefficient higher. This is probably due to the barrier layer on the poly(BTAC-MDA) composite film still containing

a few soft amide chain,^{8,9} making its permselectivity lower.

The Gas Permeability of the Heat-treated Poly(BTAC-EDA) Composite Films

Referring to Table 4, we found the α^* (CO₂/CH₄) value of the nonheat-treated poly(BTAC-EDA) composite film is less than one. This is probably due to the presence of a considerable amount of aliphatic chains (from EDA) in the barrier layer^{8,9} of the composite film caused by particularly excellent solubility for methane. This is because molecules are similar and tend to be more mutually soluble. In Table 4, the permselectivity [α^* (CO₂/CH₄) or α^* (O₂/N₂)] of the poly(BTAC-EDA) composite films increased after heat treatment. The reason for the increase in permselectivity was similar to the reason for it in the above poly(BTAC-MDA) com-

Table IV Effect of Imidization on the Gas Permeability of Poly(BTAC-EDA)^a Films Supported with PSF at 28°C

Barrier Layer	Intensity Ratio ^b :		\bar{P}^c (CO ₂)	α^* (CO ₂ /CH ₄)	\bar{P}^c (O ₂)	α^* (O ₂ /N ₂)
	$\left(\frac{\text{Imide Band at } 1775 \text{ cm}^{-1}}{\text{Aromatic C=C Band at } 1510 \text{ cm}^{-1}} \right)$					
Poly(BTAC-EDA)	0		1438	0.87	1046	2.12
Poly(BTAC-EDA) ^d	0.010		1407	2.15	995	2.46
Poly(BTAC-EDA) ^e	0.066		62.37	4.42	30.26	2.53
Poly(BTAC-EDA) ^f	0.070		6.52	4.92	4.25	3.85

^a [EDA] = [BTAC] = 0.0061M.

^b Calculated from the spectra of FTIR-ATR.

^c Barrer = 10⁻¹⁰ [cm³ (STP) cm/(s cm² cmHg)].

^d Thermal treatment: 10 min at 150°C.

^e Thermal treatment: 4 h at 135°C.

^f Thermal treatment: 6 h at 180°C.

posite film system. But the permselectivity [$\alpha^*(\text{CO}_2/\text{CH}_4)$ and $\alpha^*(\text{O}_2/\text{N}_2)$] was not high. This is probably due to the poly(BTAC-EDA) composite film still containing a considerable amount of soft aliphatic amide chains present after thermal treatment.^{8,9} Softer polymers generally have a lower diffusivity selectivity. After heat treatment, the pattern of the permeation coefficient of this composite film is $\bar{P}(\text{CO}_2) > \bar{P}(\text{O}_2) > \bar{P}(\text{CH}_4) > \bar{P}(\text{N}_2)$. As to the composite films being more permeable to CH_4 than to N_2 , this is probably due to the presence of a considerable quantity of aliphatic chains ($-\text{CH}_2-\text{CH}_2-$) in the poly(BTAC-EDA) composite film caused by particularly excellent solubility for methane.

CONCLUSIONS

In both the poly(BTAC-MDA) and poly(BTAC-EDA) composite film systems, the permselectivity of these films increased only slightly with an increasing number of coatings. In both the poly(BTAC-MDA) and poly(BTAC-EDA) composite film systems, the permselectivity [$\alpha^*(\text{CO}_2/\text{CH}_4)$ or $\alpha^*(\text{O}_2/\text{N}_2)$] of the composite films increased after heat treatment. The increase for permselectivity is attributed to two factors: (1) the softer chemical structure of amide originally contained in the composite film has reacted to become the stiffer chemical structures of imide through thermal treatment; and (2) the morphology of the composite films became denser after thermal treatment.

In the poly(BTAC-MDA) composite film system, the composite film treated at 135°C in a nitrogen atmosphere for 4 h, because the softer chemical structure of amide originally contained in the composite film has mostly reacted to form the stiffer chemical structures of imides through thermal treatment. Also, because the composite film still contains the porous PSF support, it has a high permeation coefficient [$\bar{P}(\text{CO}_2) = 44.12$ Barrer, $\alpha^*(\text{CO}_2/\text{CH}_4) = 20.51$]. The trend of the permeation coefficient of this composite film is $\bar{P}(\text{CO}_2) > \bar{P}(\text{O}_2) > \bar{P}(\text{N}_2) > \bar{P}(\text{CH}_4)$.

In the poly(BTAC-EDA) composite film system, because the composite film in it contained a considerable quantity of soft aliphatic amide after thermal treatment, the permselectivity of the composite film is not high. The trend of the permeation coefficient of this composite film is $\bar{P}(\text{CO}_2) > \bar{P}(\text{O}_2) > \bar{P}(\text{CH}_4)$

$> \bar{P}(\text{N}_2)$. This is probably due to the presence of a considerable quantity of aliphatic chains on the poly(BTAC-EDA) composite films caused by their particularly excellent solubility for methane.

The authors wish to acknowledge the financial support of the National Science Council, R.O.C.

REFERENCES

1. S. A. Stern, V. M. Shah, and B. J. Hardy, *J. Polym. Sci. Polym. Phys.*, **25**, 1263 (1987).
2. A. Iwama and Y. Kazuse, *J. Membrane Sci.*, **11**, 297 (1982).
3. K. Haraya, K. Obata, N. Itoh, Y. Shndo, T. Hakuta, and H. Yoshitome, *J. Membrane Sci.*, **41**, 23 (1989).
4. S. A. Stern, Y. Mi, H. Yamamoto, and A. K. ST. Clair, *J. Polym. Sci. Polym. Phys.*, **27**, 1887 (1989).
5. M. R. Coleman and W. J. Koros, *J. Membrane Sci.*, **50**, 285 (1990).
6. T. H. Kim, W. J. Koros, G. R. Husk, and K. C. O'Brien, *J. Membrane Sci.*, **37**, 45 (1988).
7. T. H. Kim, W. J. Koros, and G. R. Husk, *J. Membrane Sci.*, **46**, 43 (1989).
8. Y. T. Chern and L. W. Chen, *J. Appl. Polym. Sci.*, to appear.
9. Y. T. Chern and L. W. Chen, *J. Appl. Polym. Sci.*, to appear.
10. Y. T. Chern and L. W. Chen, *J. Macromol. Sci.-Chem.*, to appear.
11. H. K. Lonsdale, *J. Membrane Sci.*, **33**, 121 (1987).
12. C. R. Bartels, *J. Membrane Sci.*, **45**, 225 (1989).
13. C. R. Bartels, K. L. Kreuz, and A. Wachtel, *J. Membrane Sci.*, **32**, 291 (1987).
14. J. E. Cadotte, R. S. King, R. J. Majerle, and R. J. Petersen, *J. Macromol. Sci.-Chem.*, **A15**, 727 (1981).
15. Y. T. Chern and L. W. Chen, *J. Chin. I. Ch. E.*, to appear.
16. D. R. Paul and W. J. Koros, *J. Polym. Sci. Polym. Phys. Ed.*, **14**, 675 (1976).
17. E. Sada, H. Kumazawa, P. Xu, and M. Nishigaki, *J. Membrane Sci.*, **37**, 165 (1988).
18. K. I. Okamoto, K. Tanaka, H. Kita, A. Nakamura, and Y. Kusuki, *J. Polym. Sci. Polym. Phys.*, **27**, 2621 (1989).
19. T. Urugami, H. B. Hopfenberg, W. J. Koros, D. K. Yang, V. T. Stannett, and R. T. Chern, *J. Polym. Sci. Polym. Phys.*, **24**, 779 (1986).
20. V. T. Stannett, in *Diffusion in Polymers*, J. Crank and G. S. Park, Eds., Wiley, New York, 1971, Chap. 2.
21. D. W. Breck, *Zeolite Molecular Sieves*, Wiley, New York, 1974, Chap. 8.
22. K. C. O'Brien, W. Koros, and G. R. Husk, *J. Membrane Sci.*, **35**, 217 (1988).

Received January 25, 1991

Accepted April 24, 1991